The 2.3 Å Crystal Structure of Cholera Toxin B Subunit Pentamer: Choleragenoid

Rong-Guang Zhang*, Prakas R. Maulik†, Edwin M. Westbrook*§¶, Robert A. Reed†, David L. Scott‡, Zbyszek Otwinowski‡, Mary L. Westbrook*, and Graham Shipley†

*Division of Biological and Medical Research, Argonne National Laboratory, Argonne, Illinois 60439.

†Department of Biophysics, Boston University School of Medicine, Boston, Massachusetts 11111.

‡Department of Molecular Biophysics and Biochemistry, Yale University, New Haven, Connecticut 06511.

§Department of Biochemistry, Molecular Biology, and Cell Biology, Northwestern University, Evanston, Illinois 60602.

¶ Author to whom correspondence should be addressed.

Cholera toxin, a heterohexameric AB_5 enterotoxin released by *Vibrio cholera*, induces a profuse secretory diarrhea in susceptible hosts. Choleragenoid, the B subunit pentamer of cholera toxin, directs the enzymatic A subunit to its target by binding to GM_1 gangliosides exposed on the luminal surface of intestinal epithelial cells. We have solved the crystal structure of choleragenoid at 2.3 Å resolution by combining single isomorphous replacement with non-crystallographic symmetry averaging. The structure of the B subunits, and their pentameric arrangement, closely resembles that reported for the intact holotoxin (choleragen), the heat-labile enterotoxin from *E. coli,* and for a choleragenoid-GM_1 pentasaccharide complex. In the absence of the A subunit the central cavity of the B pentamer is a highly solvated channel. The binding of the A subunit or the receptor pentasaccharide to choleragenoid has only a modest effect on the local stereochemistry and does not perceptibly alter the subunit interface.

[1]The abbreviations used are: CT, cholera toxin; CTB, B subunit pentamer of cholera toxin; LT, heat-labile enterotoxin from *Escherichia coli*; ST, Shiga toxin; PT, pertussis toxin; VT, verotoxin; NAD, nicotinamide adenine dinucleotide; ADP, adenosine diphosphate; GM_1 (Galβ1-3GalNAcβ1-(NeuAcα2-3)4Galβ1-4Glc ceramide); cAMP, adenosine 3'5'-monophosphate; r.m.s., root-mean-square.

The profuse secretory diarrhea accompanying infection with enterotoxigenic *Vibrio cholerae* can be fatal within four to six hours *(1, 2)*. Fluid replacement remains the key to treatment since the infection spontaneously resolves within several days *(3)*. Cholera has largely been eliminated among developed nations by improved hygiene and the protection of water supplies. Among third world nations, however, cholera remains a major public health concern *(4, 5)*. Thus, efforts continue to develop a robust vaccine that will provide effective long-term immunity *(6-12)*.

The symptoms of cholera arise from the secretion of a potent bacterial enterotoxin *(7, 12-15)*. Cholera toxin is one of several microbial toxins that are composed of structurally independent A (enzymatic) and B (targeting) subunits *(16, 17)*. The refined crystal structures of the A-B toxins isolated from *Vibrio cholerae* (CT), *Escherichia coli* (heat-labile enterotoxin (LT)), *Shigella dysenteriae* (ST), and *Bordetella pertussis* (PT) have recently been reported *(18-22)*. In all four cases, the holotoxins are composed of a single A subunit tethered to the center of a pentameric ring of B subunits.

The A subunits of the AB_5 toxins are either ADP-ribosyltransferases (CT, LT, PT) or N-glycosidases (ST)*(23, 24)*. Ribosylation is a property that is shared with several other microbial toxins including the exotoxins of *Corynebacterium diphtheriae* and *Pseudomonas aeruginosa. (25, 26)* Cholera toxin, LT, and PT act at the cellular level by modifying guanine-nucleotide binding (G) proteins involved in the regulation of adenyl cyclase *(14)*. In contrast, ST and the related verotoxins (VT) inhibit protein synthesis by depurinating a specific adenosine base in 28S ribosomal RNA *(24)*.

Internalization of the A subunit is essential for intoxication *(27, 28)*. The mechanism by which this occurs is not well understood. Cholera toxin's mature A subunit consists of two chains linked by a disulfide bond. Reduction of this disulfide occurs after the toxin is bound to the target cell's surface. The liberated A1 fragment (residues 1-192 or 1-194), in the presence of NAD, ADP, and additional cytosolic factors, ribosylates $G_{s\alpha}$, a GTP-

binding regulatory protein associated with adenylate cyclase *(29-35)*. Activation of luminal sodium pumps occurs via a cAMP-dependent protein kinase *(36)*.

The B subunits of these toxins recognize and bind to specific glycolipid receptors (gangliosides) exposed on the luminal surface of epithelial cells *(37, 38)*. The B subunits of CT, LT, ST, and PT share a conserved three-dimensional fold and oligomerize to form pentameric planar rings with a central "pore". The A subunit is anchored to the pentamer by a short polypeptide that extends down into the pore *(18-22)*. In this report we describe the three-dimensional structure of cholera toxin's isolated B_5 pentamer (choleragenoid). Comparison of the crystal structures of choleragenoid, the AB_5 holotoxin (choleragen) *(18)*, LT *(20)*, and the recently published choleragenoid-GM_1 pentasaccharide complex *(39)* provides additional insights into the mechanism of action of this group of highly-evolved microbial toxins.

MATERIALS AND METHODS

Crystals of choleragenoid were grown from commercially obtained protein *(40)*. Large (0.4 mm by 0.4mm by 0.3 mm) single crystals were generally obtained within a week. The crystals were of space group $P2_1$, $a = 39.10$, $b = 94.50$, $c = 67.60$, $\beta = 96.1°$, with one pentamer in the asymmetric unit. Heavy-atom derivatives were prepared by conventional soaking techniques. Crystals were stabilized in 30% polyethylene glycol-8000, 100 mM tris, pH 7.5, with the appropriate concentration of heavy atom. Native diffraction data, and data from approximately 75 potential heavy-atom derivatives, were collected on a Siemens/Xentronics multiwire proportional-counter gas chamber area detector and processed by the Xengen computer package *(41)*. Crystals soaked in 1 mM $NaAuCl_4$ for 2 days, produced a readily interpretable Patterson difference map (Table 1). A modified version of the computer program PHARE *(42)* was used to refine five major heavy atom sites for this derivative. These sites corresponded to the pentagonal symmetry expected from the self-rotation function. A difference Fourier map calculated with the SIR

phases was readily interpretable after five-fold non-crystallographic symmetry averaging. The averaged map permitted the direct placement of the protein backbone as well as many of the amino acid side chains. Refinement by simulated annealing (X-PLOR *(43)*) and restrained least-squares methods (PROLSQ/PROFFT *(44)*) permitted the introduction of the remaining side-chains and the positioning of 199 water molecules. The current refined model contains 4,299 non-hydrogen atoms with an R-factor of 17.1% for data from 7.5 to 2.3 Å ($F > 1.5\ \sigma_F$). On average, bond lengths, bond angle distances, and planarity deviates from ideal values by less than 0.019, 0.037, and 0.038 Å, respectively. The structure of choleragen (2.5 Å resolution) was recently completed in this laboratory *(18)*. The coordinates for the other microbial toxins (choleragenoid-GM_1 complex; 2.2 Å resolution *(39)*, LT; 1.95 Å resolution *(20)*, ST; 2.5 Å resolution *(21)*, PT; 2.9 Å resolution *(22)*) and the B subunit pentamer of verotoxin-1 (2.2 Å resolution *(45)*) were obtained from the Brookhaven Protein Data Bank.

RESULTS & DISCUSSION

B Subunit Architecture

Comparison of the five representations of the B subunit comprising the single pentamer in the crystallographic asymmetric unit reveals very little deviation from exact rotational symmetry. The 103 amino acids of each B subunit are distributed among two α-helices and ten β-strands (Figure 1). Six of the β-strands form two sets of three-stranded anti-parallel sheet (Figure 2). The overall fold consists of six antiparallel β-strands forming a closed β-barrel, capped by an α-helix between the fourth and fifth strands. This long helical cap (residues 58 to 79) is gently curved with its hydrophilic face contributing to the boundary wall of the central "pore" of the B_5 pentamer (Figure 3). The B subunit's sole disulfide bridge (Cys9 = Cys86) anchors a short solvent-exposed amino-terminal helix (residues 4-12) to an interior β-strand. Ramachandran plots *(46)* reveal few unusual phi-psi angles (Figure 4).

The sequence of CTB differs from that of human-LT-1 and porcine-LT at 19 and 21 positions, respectively (80% homology) *(47-55)*. Not surprisingly, the structure of choleragenoid is very similar to that of LT (root-mean-square deviation of 0.57 Å/atom after superposition of the respective C_α backbones) *(20, 56)*. This compares favorably with deviations calculated for the intra-pentameric superposition of B subunits (0.42-0.47 Å/atom) and for superposition of the B subunits of choleragenoid and choleragen (0.59 Å/atom)(Figure 5). Notable differences between the structures of choleragenoid/choleragen and LT include a modest lengthening of the central α-helix (CT begins at residue 58 instead of residue 60). In all comparisons, sequence segments 52 through 59, 77 through 81, and the carboxyl-terminus demonstrate the most conformational variation. These areas are surface-exposed loops that refine to thermal factors suggestive of a high degree of intrinsic flexibility (Figure 6). Amino acid residues 52 to 59 form a small 'ventral' flange that participates in the recognition of the sugar ligands. The conformation of this loop becomes better defined after lactose or GM_1 pentasaccharide binding *(39, 57)*.

The B subunits of PT, ST, VT-1, and CT/LT share the same basic fold despite differences in size and low sequence homology (i.e., 103 amino acids for CTB versus 69 residues for VTB)*(20, 21, 45, 57-60)*. Deviations from the secondary structure of CTB/LTB occur primarily near the amino and carboxyl termini. For example, ST and VT-1 lack the short amino-terminal α-helix which lies at the CT/LT pentamer interface. Fifty-two of the main-chain atoms of VT-1 and LT are superposable with an r.m.s. deviation of less than 1.29 Å/atom (representing 75% of the VT-1 B chain and 50% of LTB) *(58)*. This "oligomer-binding fold" is found in several oligosaccharide and oligonucleotide-binding proteins *(61)* as well as in the monomeric nuclease from *Staphylococcus aureus (20)*.

B-Subunit Pentamer

The B subunits differ among the microbial toxins in their quaternary arrangement and in their receptor-binding specificities *(17, 62)*. The homopentamers of choleragenoid,

choleragen, LT, and ST are almost exactly five-fold symmetric with neighboring subunits related by 72 degrees of rotation. In contrast, the pertussis toxin heteropentamer is assembled from four different subunits (single copies of S2, S3, S5 and two copies of S4) and is fairly asymmetrical *(22)*. The symmetry operator for the crystalline VT-1 pentamer translates neighboring B subunits by 1.3 Å along the rotational axis *(45)*. Given that the sequences of the B subunits of ST and VT-1 are identical, it is likely that this screw axis is a crystallization artifact *(58)*. The amount of surface area buried during oligomerization differs sharply among the toxins ranging from 1269 $Å^2$ (PT S2-S4) to 2700 $Å^2$ (CT/LT). This correlates well with the observed stabilities of the respective pentamers *(63)*.

The crystalline choleragenoid is roughly cylindrical with a vertical height of 32 Å and a radius of 31 Å (Figure 3). A conical central pore, or channel, lies along the five-fold axis traversing the entire vertical height. The surfaces perpendicular to the pentameric axis are easily distinguishable. The flat dorsal surface incorporates the free carboxyl termini and the negative end of the helix dipoles *(64, 65)*. It is this surface that interacts with the A subunit in the holotoxin *(18)*. The prominent 'ventral' flange, formed by residues 50 to 64 of each subunit, creates a small pocket adjacent to the external wall of the pentamer (Figure 5). The sidechain of Trp88, which lies exposed at the base of this pocket, forms a sandwich with the terminal galactose sugar of the ganglioside in the choleragenoid-GM_1 pentasaccharide complex (Figure 6).

Choleragenoid assembly buries a large proportion of the B subunit's surface (approximately 13,000 $Å^2$/pentamer or 2700 $Å^2$/ subunit interface). Each B subunit forms approximately 30 inter-subunit hydrogen bonds and 7 salt bridges (Figure X). Choleragenoid is further stabilized by the tight interdigitation of hydrophobic groups at the subunit interface. The B pentamers of choleragenoid and the holotoxin are highly stable oligomers resistant to denaturation by chemical or thermal challenge *(66-69)*.

Residues 227 through 236 of the A2 fragment promote the cooperative assembly of choleragen *(66)*. These residues form part of a long helix that descends into the central

pore of the B subunit pentamer. Deletion of the four terminal residues of A2 (residues 236 through 240) weakens the A/B interaction without impairing pentamer formation. The tethering and template functions of the A2 chain are not unexpected given its intimate interface with the B subunits lining the pore. Oligosaccharide binding prevents the dissociation of choleragenoid observed at low pH (< 4) and improves the pentamer's thermal stability *(70-72)*. The additional stability is not dependent on a major structural rearrangement (< 3-4% change in β-sheet or α-helix content) *(71)*.

The Central Pore (Doughnut Hole)

One of the striking architectural features of the AB_5 toxins is the presence of a central pore or channel that runs along the five-fold axis (Figure 7). The boundaries of these conical pores are established by long, closely-packed, parallel α-helices. These helices run the length of the pore and gently bow inward during their course reducing the diameter of the pore from 16 Å (amino end) to 11 Å (carboxyl end).

The sidechains of Asp59, Lys62, Lys63, Glu66, Arg67, Asp70, and Arg73 extend into the central pore with five-fold redundancy. The sequential alternation of positive and negative charges ensures optimal stabilization of neighboring helices by salt bridges and results in a pore with a modest net positive charge. Holotoxin cannot be reconstituted by mixing A subunits and preformed choleragenoid *in-vitro (68)*. The pore may be simply too narrow or electrostatically inhospitable to permit entry of the A2 chain. The amino-acids lining the pore are identical in CT and LT with the exception of the substitution of an Asn for Asp70 in some CT strains. The A/B interface of Shiga toxin is much different with the pore walls consisting entirely of hydrophobic residues (Asn35, Ser38, Ser42, Ile45, and Thr46) *(21)*.

The carboxyl-terminus of the A2 chain (residues 212-240) occupies the cental pore of the holotoxin. The conformation of this 'anchoring' segment is α-helical in CT *(18)* and ST *(21)*, while in LT this segment is predominantly extended chain with a small terminal

helix *(20)*. The A2 chain is replaced in the crystal structure of choleragenoid by multiple well-resolved water molecules. The additional solvent encourages favorable intersubunit interactions among B-pentamer sidechains and presumably accounts, at least in part, for the extremely high stability of choleragenoid *(67-69, 73)*.

Photolabelling and surface pressure experiments indicate that the B subunits do not deeply penetrate into the membrane while bound to their ganglioside receptors *(74-77)*. Binding is, however, associated with an increase in membrane permeability. The holotoxin and choleragenoid, but not the A subunit, increase the permeability of GM_1-containing liposomes *(77)*. Krasilnikov *et al.*, 1991 reported that at pH 4.5 CTB forms an anionic channel with a mean conductance that varies inversely with pH *(78)*. Using small molecular probes, the effective diameter of the channel was calculated to be 2.1 +/- 0.2 nm. This value is similar to estimates made from low-resolution electron micrographs of CT bound to lipid films *(79-81)*. One explanation for the discrepancy between this diameter and that measured from the crystalline toxins (an effective diameter of 11-16 Å depending upon the depth of insertion) is that the pore widens after membrane attachment. This would be consistent with the A subunit translocating into the cytoplasm by unfolding and threading its way through the central pore *(30,31)*. However, there is no structural evidence to support such a dramatic rearrangement of the pentamer interface.

The Oligosaccharide Binding Site

Cholera toxin productively binds to GM_1 gangliosides (Galβ1-3GalNAcβ1-(NeuAcα2-3)4Galβ1-4Glc ceramide). Fucosylated derivatives of GM_1 (a fucose residue, α-glycosidically linked to the 2-position of the terminal galactose) may also serve as receptors *(82)*. The association constants of CT with GM_1 or Fuc-GM_1 gangliosides, as determined by high-sensitivity isothermal titration calorimetry, are comparable ($1.9 \times 10^7\ M^{-1}$ and $4 \times 10^7\ M^{-1}$, respectively at 25 °C). The saccharide moiety of GM_1 binds to the AB_5 hexamer and the B-pentamer but not to the isolated B subunits *(83)*.

Each receptor-binding site is derived primarily from the residues of one B-subunit *(39)*. The GM_1 pentasaccharide binds within a pocket formed by Glu11, Tyr12, His13, Asn14, Glu51, Gln56, His57, Gln61, Trp88, Asn90, and Lys91. Comparison of the crystal structure of choleragenoid with that of the GM_1 pentasaccharide complex *(39)* reveals only modest local conformational changes (Figure 8). The coordinates of the respective alpha-carbon traces superpose with a r.m.s. deviation of less than 0.5 Å/ C_α atom. Movement of the peptide backbone of the residues forming the pocket itself, however, is slightly greater (r.m.s. = 0.74 Å/C_α atom; 0.40 Å/C_α atom if Gln56, His57, and Gln61 are excluded). The most consistent change in backbone structure is the reorientation of the His13-Asn14 peptide bond which flips in the pentasaccharide complex to permit a water-mediated hydrogen-bond from O13 to the sialic acid..Careful analysis also reveals a small (< 1 Å) *en bloc* shift of residues 54 through 64 towards the saccharide, narrowing the pocket and presumably further anchoring the receptor.

In the absence of ligand, the conformation of the binding site appears to be fairly flexible with each subunit in the crystalline pentamer slightly different. Even at the side-chain level, however, only a modest repositioning of choleragenoid's amino-acid sidechains is necessary in order to accomodate the oligosaccharide. The pentasaccharide forms direct or water-mediated hydrogen bonds with the sidechains of Asn14, Glu51, Gln61, Trp88, Asn90, and Lys91.

GM_1 gangliosides promote the cooperative folding of the B pentamer *(71, 84, 85)*. Thermal stability is improved with unfolding shifted from 66 °C to 87 °C *(71)*. Schon and Freire *(72)* calculated a cooperative free energy of -850 cal/mol in the presence of GM_1 divided into an enthalpy of -11 kcal/mol and an entropy of -35.7 cal/K-mol. A small conformational change accompanying GM_1 binding has been inferred from circular dichroism spectra and by the increased ability of A subunits to associate with intact pentamer when the pentamer is bound to GM_1 at the cell surface *(86)*. Similar experiments

using Fourier-transform infrared spectroscopy, however, have shown little, if any, change in the secondary structure *(71)*.

Cholera toxin binds to GM_1 with a Hill coefficient of 1.2 *(87)*. The source of this cooperativity is not obvious from the crystal structures. The bound pentasaccharide forms a single solvent-mediated hydrogen bond with the backbone nitrogen of a a neighboring subunit's Gly33 *(39)*. Amino acid substitutions at position 33 that are negatively-charged or hydrophobic (Glu, Asp, Ile, Val, Leu) markedly reduce the affinity for GM_1, whereas small or positively-charged substitutions (Ala, Lys, Arg) have little effect *(88)*. Two adjacent residues (Lys34 and Arg35) are not mutationally sensitive. Curiously, Gly33 is fairly remote from the binding pocket and its contribution to the binding energy presumably weak. The residue's importance may be related to the stabilizing hydrogen-bond formed between its carbonyl oxygen and the hydroxyl group of Tyr12. The precise positioning of Tyr12 is important for two reasons; (1) one edge of the tyrosine ring contacts the pentasaccharide's sialic acid, and (2) hydrogen bonds from the peptide backbone of neighboring residues (Glu11O, His13O, and His13N) anchor the sialic acid. In the absence of ligand, the solvent-exposed loop that includes residues 11 through 15 appears to be fairly flexible (Figure 5). Amino-acid substitutions at sequence position 33 may, therefore, affect ganglioside binding by compromising the stability of Tyr12.

The crystalline binding pockets of CT and LT *(20)* appear to be identical. The contributing amino acids are conserved with the possible exception of residue 13, which is a histidine in CT but may be either a histidine or arginine in LT depending on the strain of *E. coli* from which the toxin is isolated *(51-54)*. The side-chain of His13 does not directly participate in the binding of the GM_1 pentasaccharide. Thus, it is difficult to explain the disparity in receptor binding specificities of CT and LT. Comparable binding sites have not yet been identified for the Shiga family of toxins *(89-92)*. These toxins differ from CT and LT in preferring the globotriosylceramides G_{b3} and G_{b4} *(93)*.

The mechanism by which the A1 fragment crosses the membrane into the cytoplasm also remains a mystery. The structure of the choleragenoid-GM_1 pentasaccharide complex *(39)* argues for the holotoxin binding to the membrane with the A subunit pointing away from the cell *(20, 39)*. This orientation is supported by recent immunological experiments indicating that the A1 fragment of the surface-bound or surface-assembled holotoxin is accessible to anti-A1 antibodies *(94)*. Given the structural stability of the B pentamer, it is unlikely that the pentamer dissociates to provide a larger pore for passage of the A1 subunit. Internalization of the toxin must, therefore, be dependent upon some form of endocytosis that is perhaps mediated by the KDEL terminus of the A2 chain *(95-96)*. Cholera toxin coupled to horse-radish peroxidase (HRP) was visualized in the Golgi-endoplasmic reticulum-lysosomal system of cultured cells within 1 hour of incubation at 37 °C. The entry of the toxin-HRP conjugate appeared not to occur through coated pits and was negligible at 4 °C *(97-99)*.

Vaccine Development

In the past, parenterally administered cholera vaccines have failed to produce a strong mucosal response. Recent efforts have focused on the development of oral vaccines that can stimulate protective IgA within the intestinal lumen *(10, 100)*. Most protein antigens that are good parenteral immunogens are poorly immunogenic when given orally *(101)*. Cholera toxin is an exception *(102, 103)*. Choleragenoid has also been shown to act as a mucosal adjuvant; i.e., it can stimulate immunity to unrelated protein antigens delivered with it to a mucoal surface *(104)*. Because of the toxicity of the holotoxin, investigators have focused on the vaccine potential of choleragenoid *(105)*. Isolated cholera toxin B subunits can confer limited protection for up to six years, still considerably better than the 3-6 month coverage provided by the older parenteral vaccines.

Ganglioside binding is important to the immunogenticity and adjuvant properties of CT *(106-108)*. Members of the cholera enterotoxin family contain at least 20 epitopes that are recognizable by checkerboard immunoblotting. An epitope that includes Ala46 appears to

be particularly important. This epitope is common to CTB and human-LT but not porcine-LT and is not blocked by binding of the toxin to GM_1 gangliosides. Ala46 is part of a highly exposed surface loop (residues 40-48) that lies on the 'dorsal' edge of the pentamer adjacent to the A subunit of the holotoxin.

Shoham *(109)* studied the structure of a 15 amino acid peptide corresponding to an immunogenic loop on the B subunits of CT and LT (amino acids residues 50 through 64: VEVPGSQHIDSQKKA). A monoclonal antibody raised against this peptide cross-reacts with CT in a solid-phase immunosorbent assay *(110-111)*. The conformation of the peptide in the crystalline Fab-peptide complex (2.3 Å resolution) is markedly different from that observed in either CT or LT (Figure 9). The peptide superposes onto the corresponding segment of choleragenoid with a r.m.s. deviation of 4.6 Å for C_α atoms 52 through 63. Elimination of residues 52 and 61 through 63 improves the superposition considerably (r.m.s. = 2.33 Å). The conformation of three of the amino-terminal residues (VPG), however, are virtually identical (r.m.s. of 0.05 Å/atom). The development of adequate peptide vaccines for cholera may require the synthesis of peptides that are constrained to retain the conformation of the epitope.

Acknowledgements: The coordinates will be deposited in the Brookhaven Protein Data Bank. We wish to thank Dr. Paul B. Sigler of Yale University for generously providing computational and graphics facilities during a portion of this work.

Table 1. Single isomorphous replacement (SIR) of choleragenoid.

Structure	Resolution (Å)								
Parameter	11.71	8.28	6.40	5.22	4.40	3.81	3.36	3.00	Overall
Figure of Merit[1]	0.31	0.58	0.56	0.53	0.48	0.47	0.42	0.30	0.43
Phasing Power of Derivative[2]									
$NaAuCl_4$	1.07	3.56	4.25	3.65	2.45	2.26	1.89	1.35	2.01

[1]Figure of merit is a measure of the relative reliability of a phase based on the consistency of the SIR analysis. The maximum value is 1.0.

[2]$\Sigma |F^c_h| / [|F^o_p| \exp(i\theta_c) + F^c_h| - |F^o_{ph}|]$, where $|F^c_h|$ is the calculated diffraction amplitude of the heavy atom, $|F^o_p|$ and $|F^o_{ph}|$ are the observed amplitudes for the protein and heavy-atom derivative, respectively; θ_c is the calculated phase, and the sum is over all observations.

Figure 1. Sequence and secondary structure of the cholera toxin B subunit *(46-54)*. Automated sequencing of polymerase-chain reaction generated amplicons has identified three types of B subunits in CT 01 strains *(51)*. The sequence shown here is consistent with that determined from the crystal structure. Since the five B subunits have been independently refined, minor variations in the assignment of secondary structure occur in the individual B subunits *(112)*. Residues implicated as either being important to pentamer stability or to ganglioside binding are indicated with filled squares and ovals, respectively. Basic residues (Arg, Lys, His) are shown in blue and acidic residues (Asp, Glu) in red. The sequence of the highly homologous heat-labile enterotoxin from *E. coli* is included for comparison (asterisks denote residues identical to that of cholera toxin).

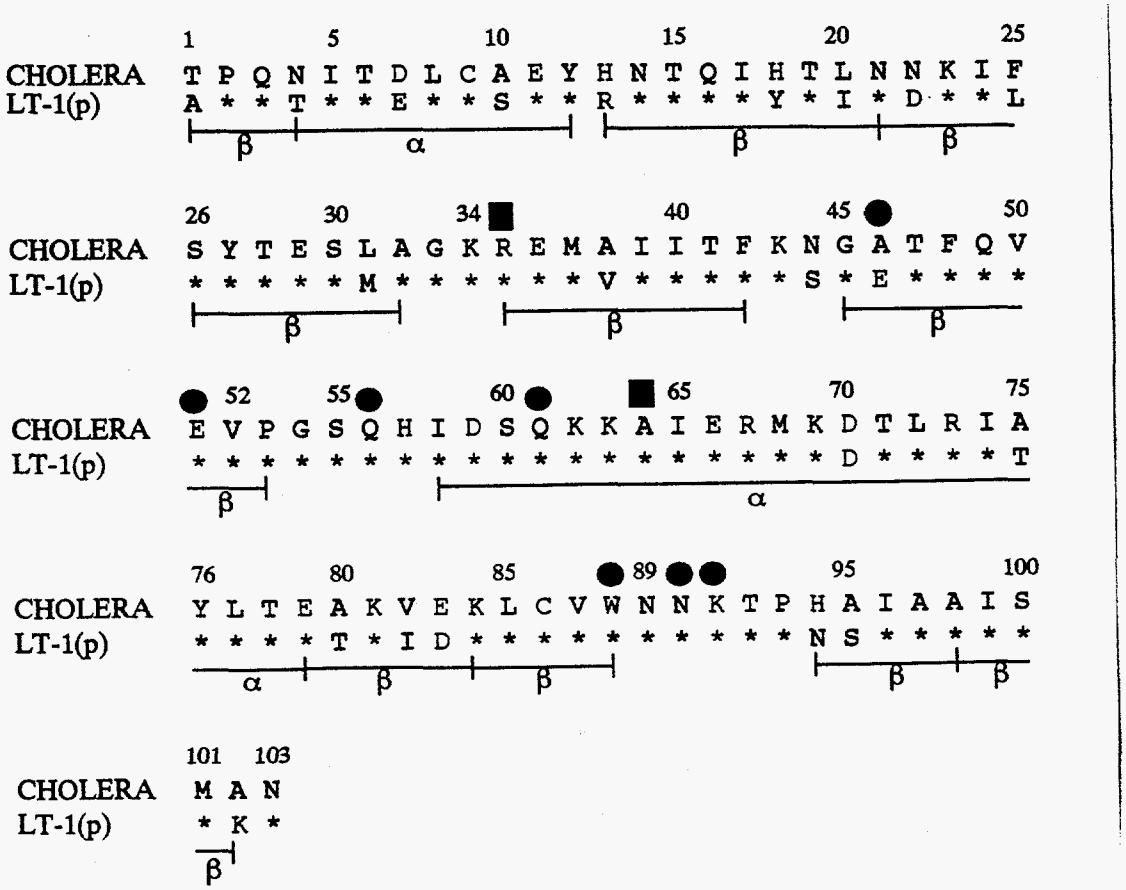

Figure 2. Pentamer formation: electron-density map and schematic illustration of the interaction between B subunits. (A) A $2F_O$ - F_C map of the interface between two adjacent B subunits near the ganglioside-binding site. Three β-strands from each of the two subunits combine to form an extended six-stranded β-sheet. The interactions shown here are typical of those seen in the four other representations in the pentamer. The map is contoured at 1 σ. (B) Schematic rendition of two adjacent B subunits. Pentamer formation depends only on interactions between nearest neighbors. The ganglioside-binding pocket lies at the interface of two subunits adjacent to Trp88.

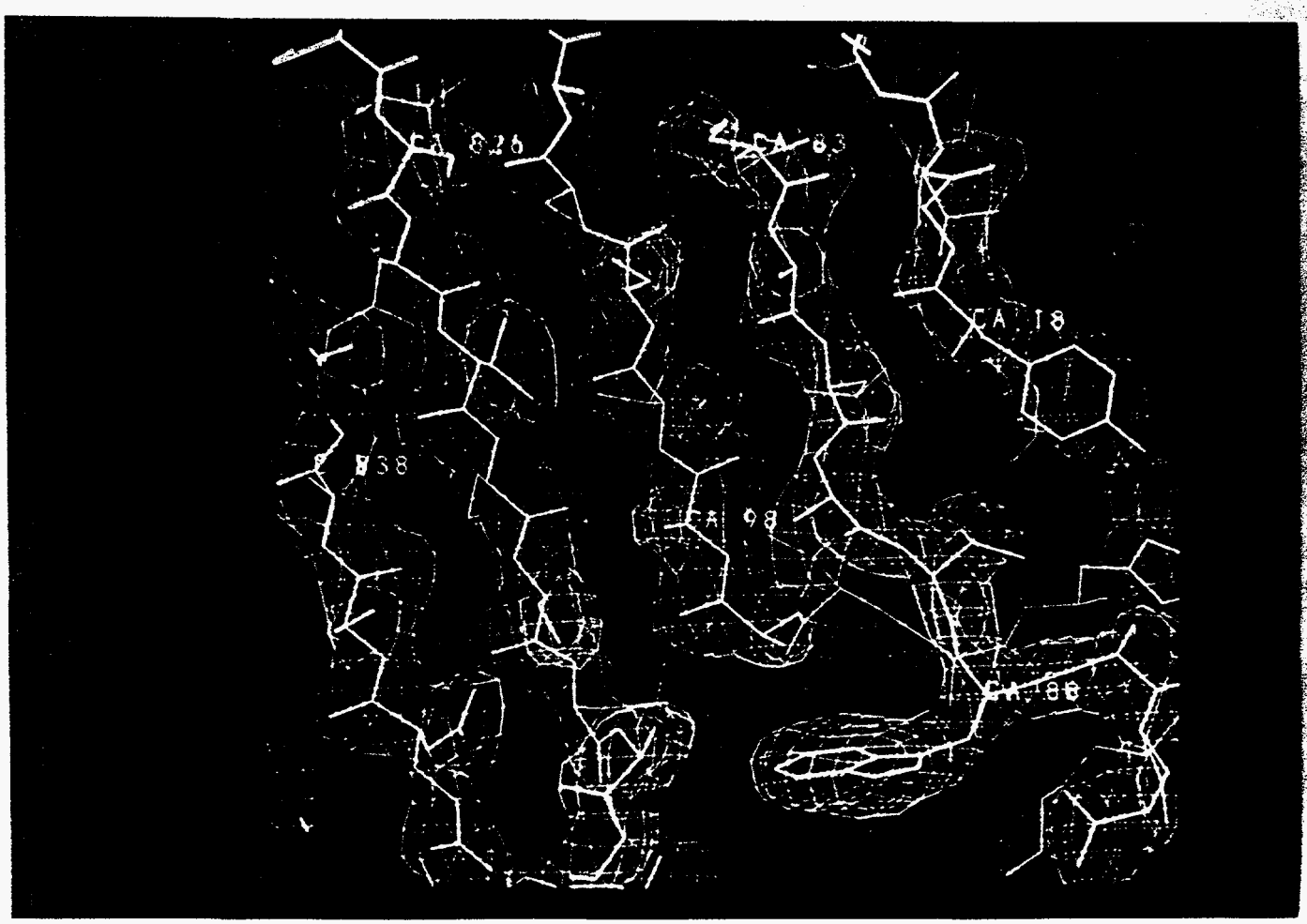

Figure 2.B

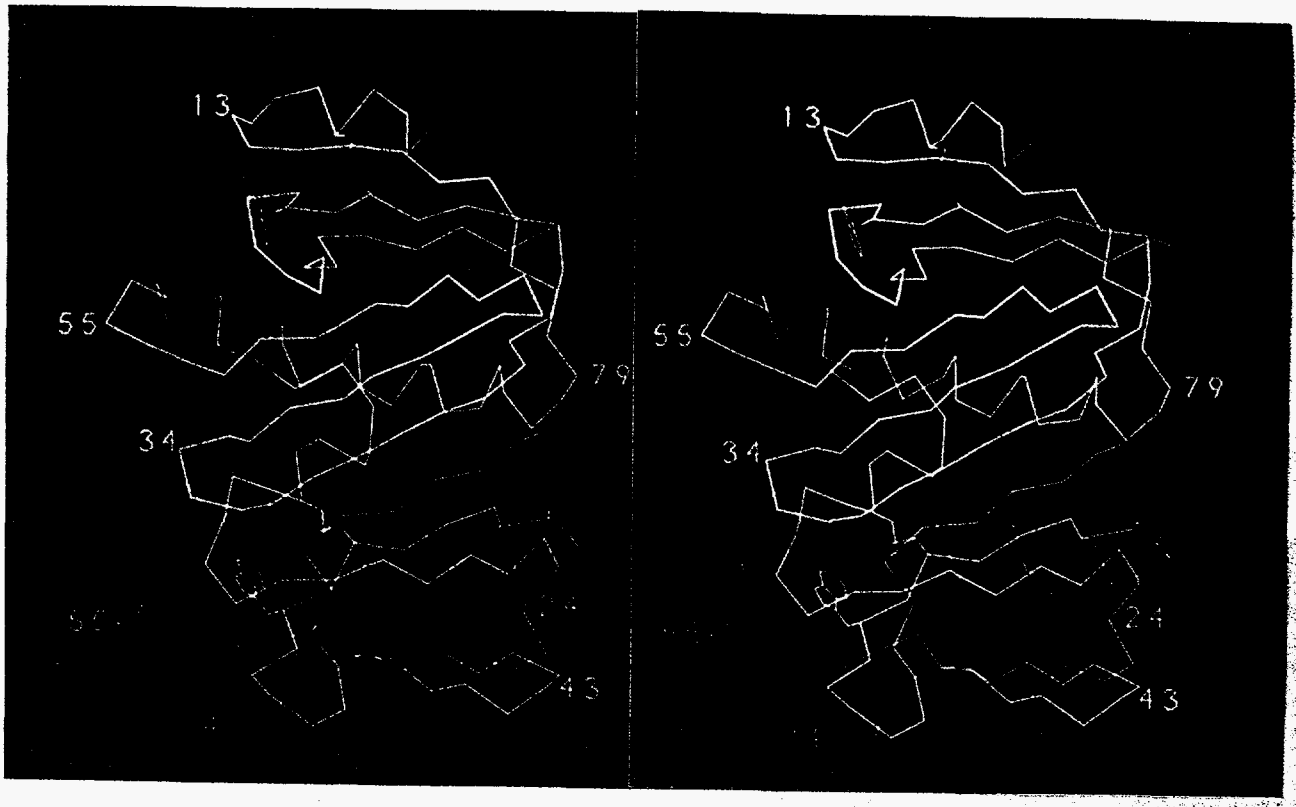

Figure 3. Overview of the crystalline choleragenoid. (A) Stereopair of the pentamer viewed from the 'side' (along an axis perpendicular to the five-fold axis). Each subunit is colored differently with only the side-chains of Tyr12, Gln56, and Trp88 shown (green). These residues surround the GM_1-binding sites located adjacent to the 'ventral' flange of choleragenoid. The A subunit in the holotoxin lies atop the 'dorsal' surface. The disulfide bridges between residues 9 and 86 are colored magenta. The amino and carboxyl termini are shown as blue and red spheres, respectively. **(B)** Stereopair and corresponding space-filling representation (C) of the pentamer viewed from the 'ventral' surface (along an axis parallel to the five-fold). Residues are indicated as in (A). The central pore of choleragen is occupied by the helical terminus of the A2 chain in the holotoxin *(18)*.

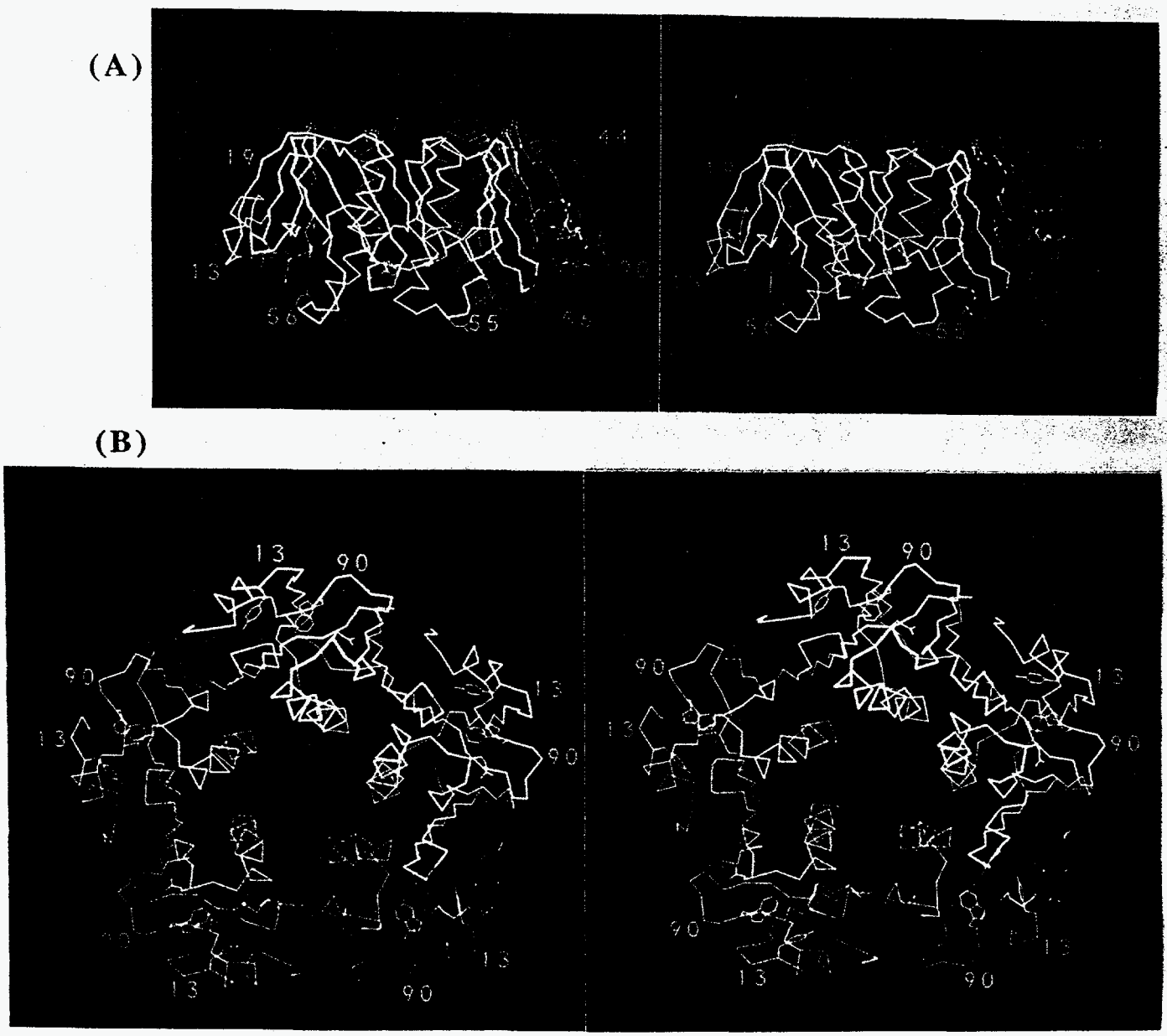

(C)

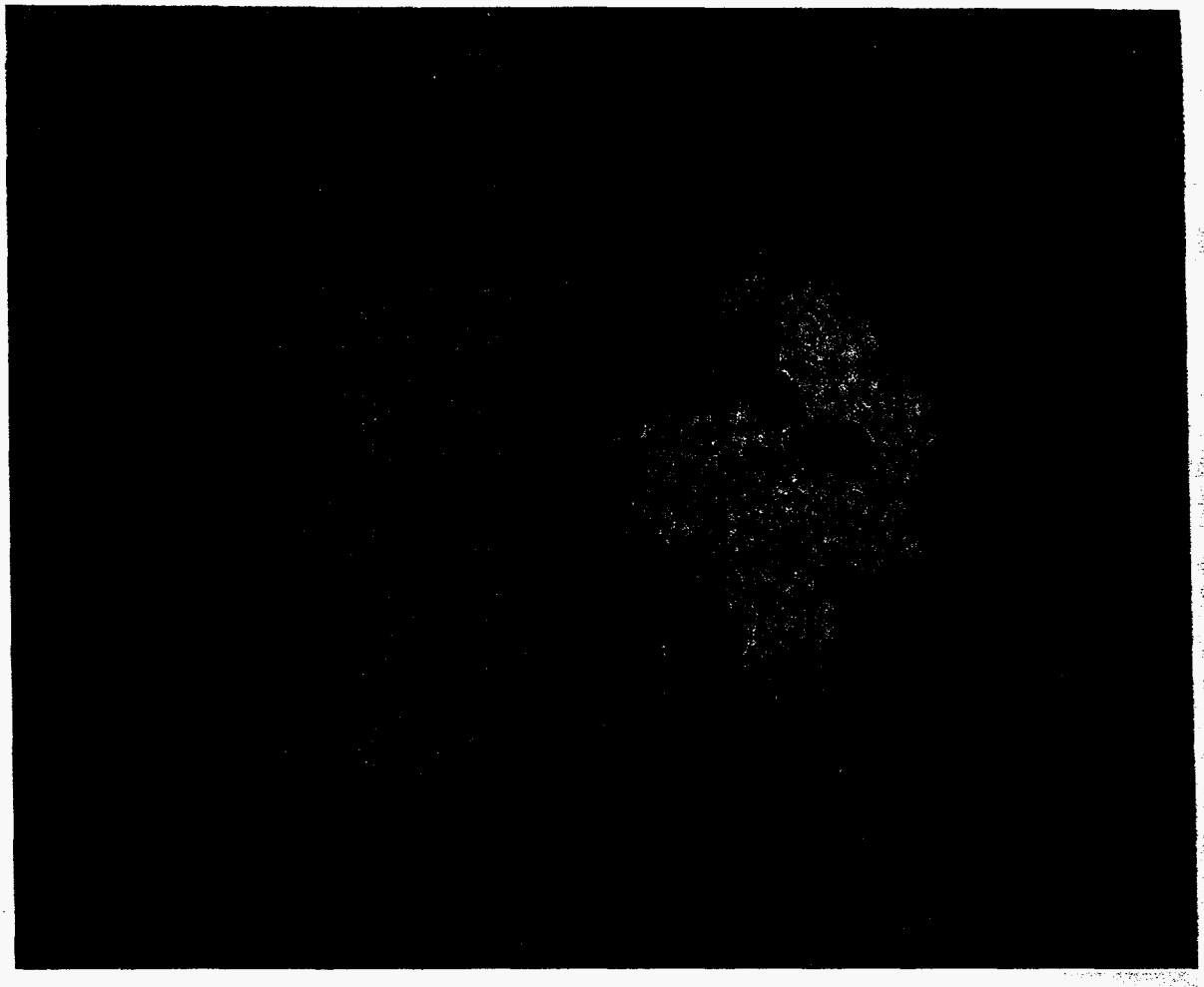

Figure 4. Ramachandran plot for the 103 amino acids of a representative B subunit from the crystalline structure of choleragenoid *(45)*. Phi-psi angles for glycine amino-acids are indicated by circles; all other amino-acid types are represented by crosses. The three outlying residues (Gly45, Asp59, and Lys81) lie within solvent-exposed loops that appear to be conformationally flexible (Figure 5).

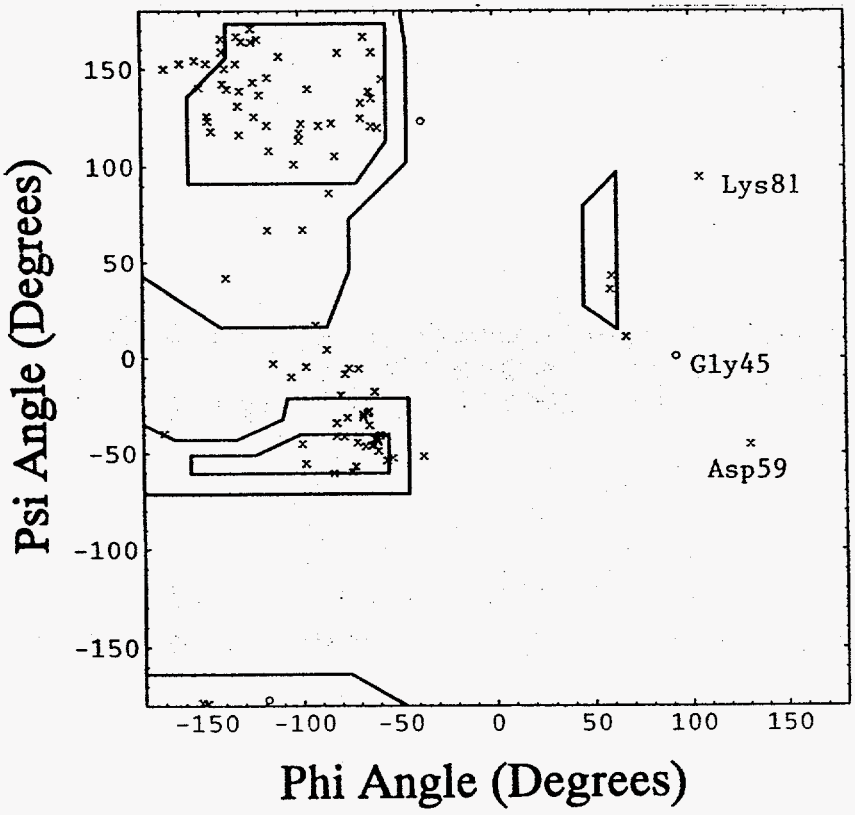

Figure 5. Conformational variability among the cholera family of toxins. Superposition of the alpha-carbon trace of a B subunit of choleragenoid on the trace of a second B subunit of the choleragenoid pentamer (black), a B subunit from choleragen (violet: dashed line) *(18)*, a B subunit from the choleragenoid-GM_1 pentasaccharide complex (red)*(39)*, and a B subunit from LT (blue)*(20)*. The most positional variation occurs in a surface-exposed loop (residues 50 through 64), and at the amino and carboxyl termini.

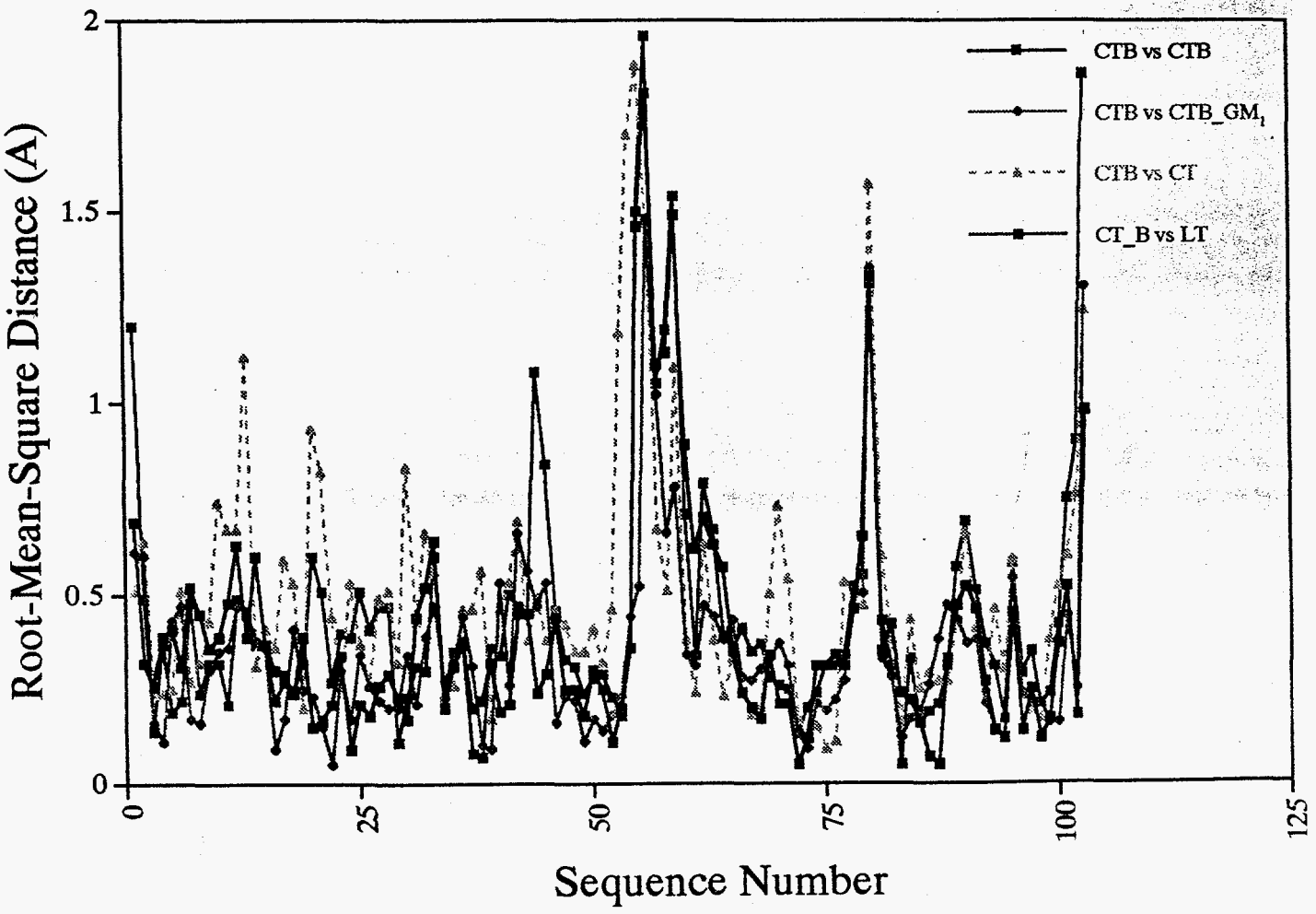

Figure 6. Refined isotropic temperature factors for a representative B subunit of choleragenoid (C_α atoms). The temperature factors of the other four B subunits that form the single pentamer in the crystallographic asymmetric unit follow a similar distribution. The molecular average is indicated by the horizontal dashed line.

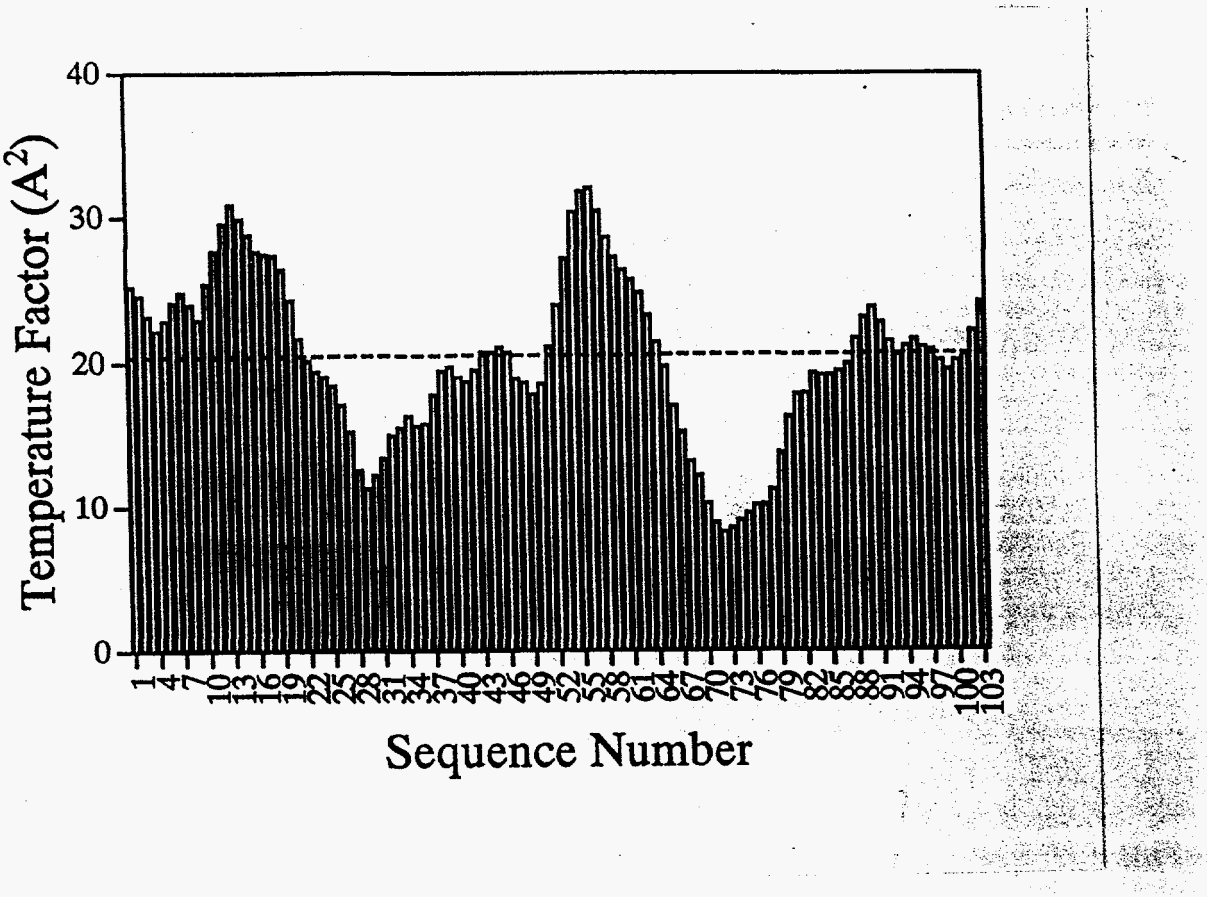

Figure 7. The central pore of choleragenoid and choleragen. Cross-section through the central pore of (A) choleragenoid, and (B) choleragen along the five-fold axis. The side-chains of only the central α-helices are shown for clarity. Solvent molecules are indicated as yellow spheres. The carboxyl end of the A2 chain (gold) occupies the central pore of choleragen. Part of the A1 chain (cyan) is also shown in (B) for orientation. In the absence of the A2 chain, the pore becomes a highly-solvated channel. The number of solvent molecules in both crystal structures may be underestimated as a result of the limited resolution.

(A)

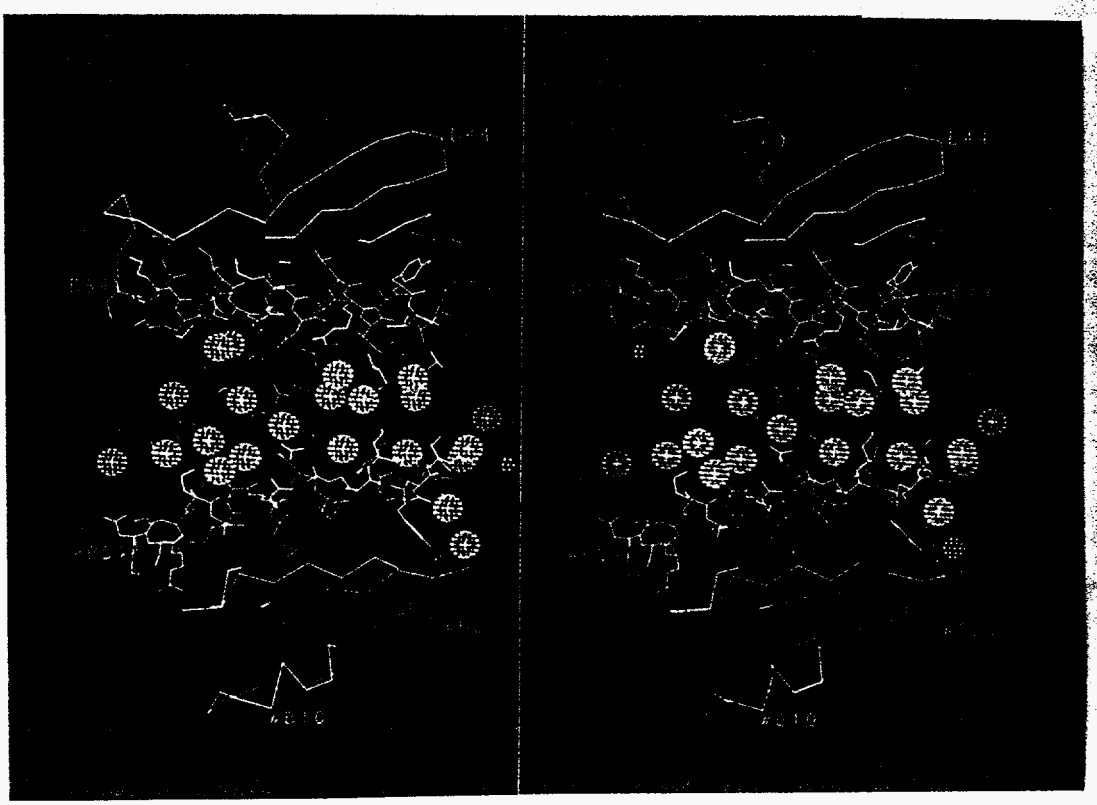

Figure 7.B

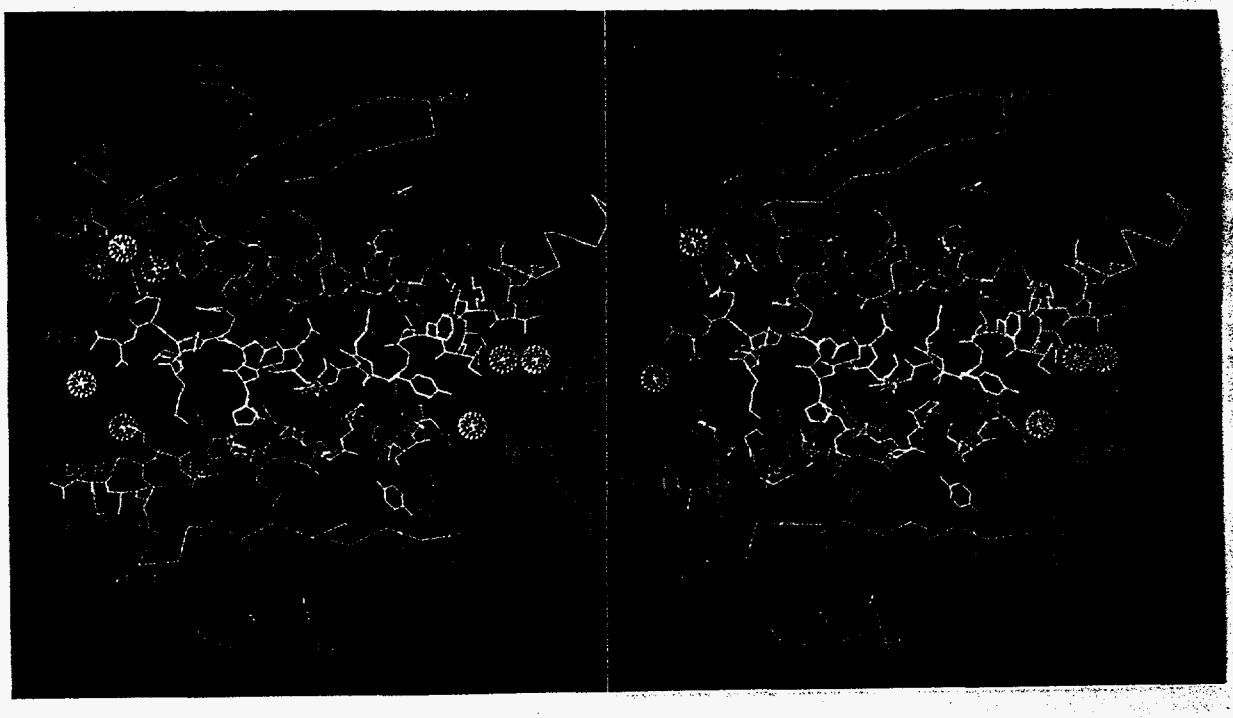

Figure 8. Schematic representation of the ganglioside-binding site of cholera toxin in the absence (A) and presence (B) of a GM_1 pentasaccharide *(39).* GM_1 (1,284 kD) is a ceramide linked by a β-glycosidic bond to a polysaccharide. The ganglioside is an integral membrane component with a polar head group (the polysaccharide) extending out of the membrane, and two hydrocarbon tails (the ceramide), extending into the hydrophobic layer of the membrane *(113, 114).* Physical studies of the interaction of choleragenoid with GM_1 (fluorescence spectroscopy, photoaffinity labelling, differential calorimetry, differential solubility thermal gel analysis, nuclear magnetic resonance, hydrodynamics) are consistent with the location determined by X-ray crystallography. The five-fold redundant receptor-binding sites are located on the 'ventral' surface of the pentamer opposite the surface that interacts with the A subunit. The binding pocket appears to be 'hardwired' requiring very little adjustment of either sidechains or backbone to coordinate GM_1. Residues interacting with the pentasaccharide are all derived from a single subunit with the exception of Gly33 (cyan). Water molecules are indicated as yellow spheres (W).

(A)

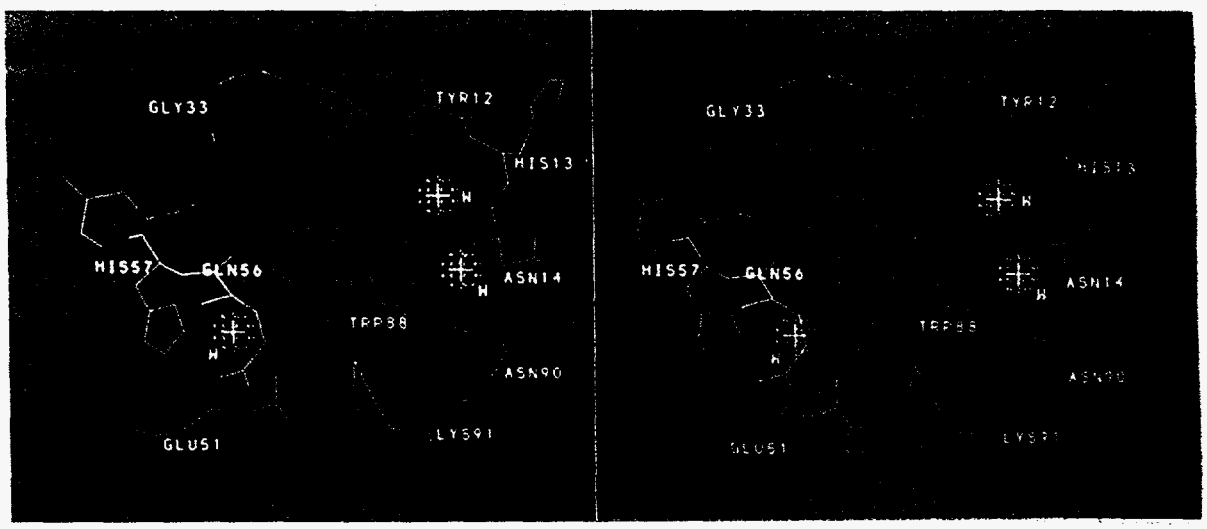
GLY33
TYR12
HIS13
H
HIS57
GLN56
H
ASN14
H
TRP88
H
ASN90
GLU51
LYS91
GLY33
TYR12
HIS57
GLN56
ASN14
TRP88
GLU51

(B)

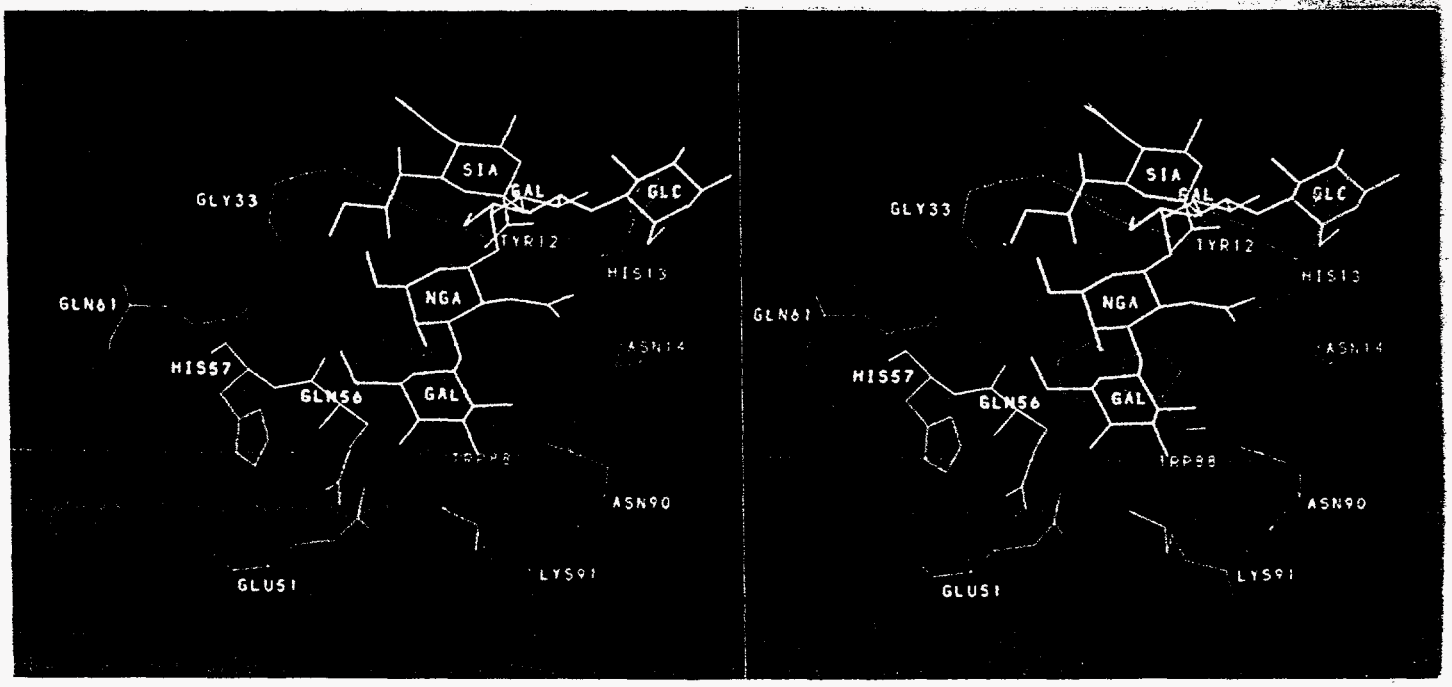
SIA
GAL
GLC
GLY33
TYR12
HIS13
GLN61
NGA
ASN14
HIS57
GLN56
GAL
ASN90
GLU51
LYS91
SIA
GAL
GLC
GLY33
TYR12
HIS13
GLN61
NGA
ASN14
HIS57
GLN56
GAL
ASN90
GLU51
LYS91

Figure 9. Superimposition of the coordinates of an immunogenic CT peptide. Residues 50 to 64 of CT, which lie near the ganglioside-binding pocket, constitute a highly immunogenic peptide *(109-111)*. Immunization of laboratory animals with the purified peptide (VEVPGSQHIDSQKKA) induces partial protection from cholera. The structure of the peptide has been determined as it exists in the intact protein (blue) and as it appears in a complex with the Fab fragment of a monoclonal antibody (red). The peptides were superimposed using the backbone atoms of residues 7 through 10 with a root-mean-square deviation of 0.65 Å/ C_α atom. The segment containing residues 3 to 5 is very similar (r.m.s. = 0.05 A). No electron-density was found for residues 1, 2 and 15 in the peptide-Fab complex.

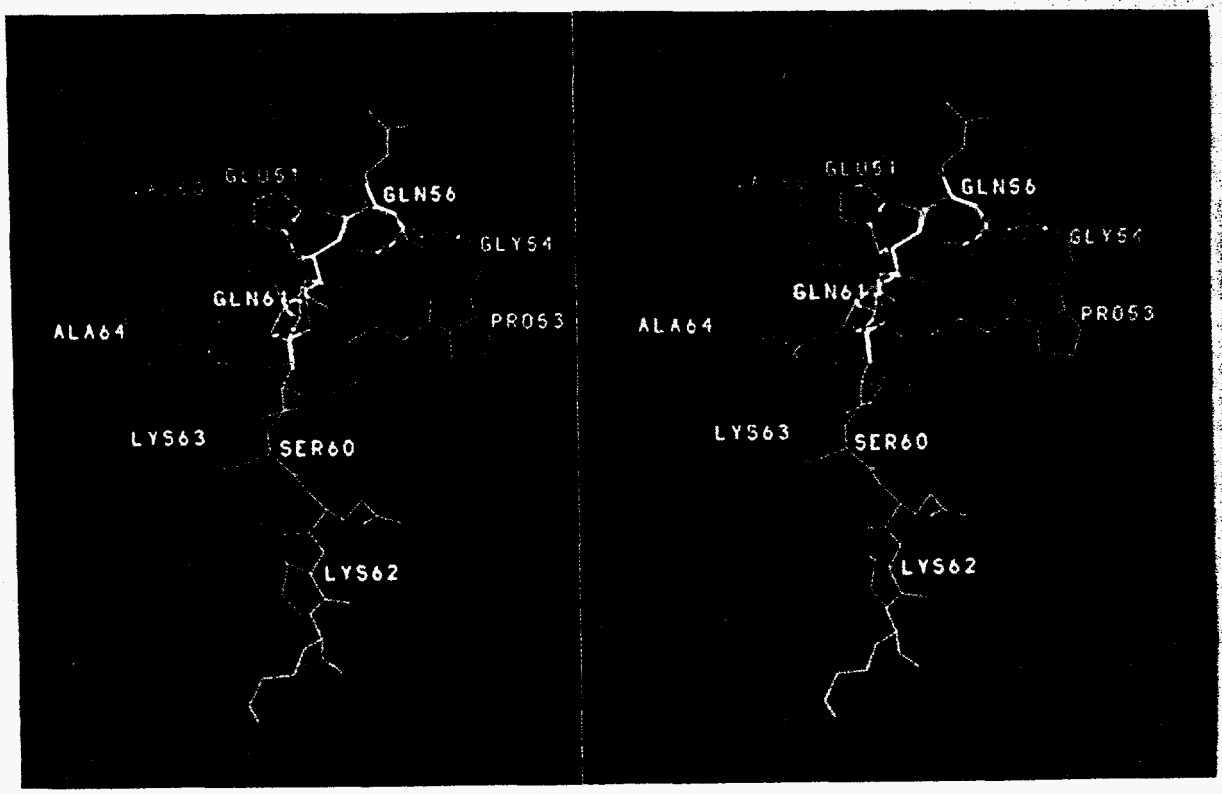

References:

1. Black, R.E. (1986) In: *Developments of Vaccines and Drugs against Diarrhea*, 11th. Nobel Conf. Stockholm 1985 (Holmgren, J., Lindberg, A., and Mollby, R. eds) Studentlitteratur, Lund, Sweden, 23-32.
2. Field, M., Rao, M.C., and Chang, E.B. (1989) *New Engl. J. Med.* **321**, 879-883.
3. Hirschorn, N., and Greenough, W.B. III, (1991) *Sci. American* **264**, 16-22.
4. Glass, R.I., Libel, M., Brandling-Bennett, A.D. (1992) *Science* **256**, 1524-1525.
5. Maddox, J. (1991) *Nature* **350**, 640.
6. Arnon, R. (1991) *Molec. Immun.* **28**, 209-212.
7. Nashar, T.O., Amin, T., Marcello, A., and Hirst, T.R. (1993)*Vaccine* **11**, 235-240.
8. Finkelstein, R.A. (1992) *Science* **257**, 852.
9. Holmgren, J. (1990) *Curr. Sci.* **59**, 665-668.
10. Manning, P.A. (1992) *Vaccine* **10**, 1015-1021.
11. Clemens, J.D., Sack, D.A., Harris, J.R., Van Loon, F., Chakraborty, J., Ahmed, F., Rao, M.K., Khan, M.R., Yunus, M.D., Huda, N., Stanton, B.F., Kay, B.A., Walter, S., Eeckels, R., Svennerholm, A-M., & Holmgren, J. (1990) *Lancet* **335**, 270-273.
12. De, S.N. (1959) *Nature* **183**, 1533-1534.
13. Black, R.E., Levine, M.M., Clemens, J.D., Young, C.R., Svennerholm, A.-M., and Holmgren, J. (1987) *Infect. Immun.* **55**, 1116-1120.
14. Cassel, D., and Pfeuffer, T. (1978) *Proc. Natl. Acad. Sci. USA* **75**, 2669-2673.
15. Finkelstein, R.A., in *Immunochemical and Molecular Genetic Analysis of Bacterial Pathogens*, P. Owen and T.J. Foster, Eds. (Elsevier Science Publishers, New York, 1988) vol. 85.
16. Spangler, B.D. (1992) *Microbio. Reviews* **56**, 622-647.
17. Burnette, W.N. (1994) *Structure* **2**, 151-158.
18. Zhang, R.-G., Scott, D.L., Westbrook, M.L., Nance, S., Spangler, B.D., and Westbrook, E.M. (1994) Submitted to *Proceedings National Academy, U.S.A.*.
19. Sixma, T.K., Pronk, S.E., Kalk, K.H., Wartna, E.S., Van Zanten, B.A.M., Witholt, B., and Hol, W.G.J. (1991) *Nature* **351**, 371-378.
20. Sixma, T.K., Kalk, K.H., van Zanten, B.A.M., Dauter, Z., Kingma, J., Witholt, B., Hol, W.G.J. (1993) *J. Mol. Biol.* **230**, 890-918.
21. Fraser, M.E., Chernaia, M.M., Kozlov, Y.V., and James, M.N.G. (1994) *Structural Biology* **1**, 59-64.
22. Stein, P.E., Boodhoo, A., Armstrong, G.D., Cockle, S.A., Klein, M.H., and Read, R.J. (1994) *Structure* **2**, 45-57.
23. Moss, J., and Vaughan, M. (1988) *Advan. Enzymology* **61**, 303-379.
24. O'Brien, A.D., and Holmes, R.K. (1987) *Microbiol. Rev.* **51**, 206-220.
25. Foster, J.W., and Kinney, D.M. (1985) *CRC Critical Review in Microbiology* **11**, 273-298.
26. Wick, M.J., Frank, D.W., Storey, D.G., and Iglewski, B.H. (1990) *Ann. Rev. Microbiol.* **44**, 335-363.
27. Janicot, M., Fouque, F., and Desbuqois, B. (1991) *J. Biol. Chem.* **266**, 12858-12865.
28. Houslay, M.D., and Elliott, K.R.F. (1981) *FEBS Lett.* **128**, 289-292.
29. Kahn, R.A., and Glman, A.G. (1984) *J. Biol. Chem.* **259**, 6228-6234.
30. Gill, D.M. (1975) *Proc. Natl. Acad. Sci. U.S.A.* **72**, 2064-2068.
31. Gill, D.M., and Coburn, J. (1987) *Biochem.* **26**, 6364-6371.
32. Galloway, T.S., and van Heyningen, S. (1987) *Biochem. J.* **244**, 225-230.
33. Kassis, S., Hagmann, J., Fishman, P.H., Chang, P.P., and Moss, J. (1982) *J. Biol. Chem.* **257**, 12148-12152.
34. Lee, C.-M., Chang, P.P., Tsai, S.-C., Adamik, R., Price, S.R., Kunz, B.C., Moss, J., Twiddy, E.M., and Holmes, R.K. (1991) *J. Clin. Invest.* **87**, 1780-1786.
35. Serafini, T., Orci, L., Amherdt, M., Brunner, M., Kahn, R.A., and Rothman, J.E. (1991) *Cell* **67**, 239-253.
36. Peterson, W.J., and Ochoa, L.G. (1989) *Science* **245**, 857-859.
37. Fishman, P.H., Pacuszka, T., and Orlandi, P.A. (1993) *Advances in Lipid Research* **25**, 165-187.
38. Hansson, H.-A., Holmgren, J., and Svennerholm, L. (1977) *Proc. Natl. Acad. Sci. U.S.A.* **74**, 3782-3786.
39. Merritt, E.A., Sarfaty, S., van den Akker, F., L'hoir, C.L., Martial, J.A., and Hol, W.G.J. (1994) *Protein Sci.* **3**, 166-175.
40. Maulik, P.R., Reed, R.A., and Shipley, G.G. (1988) *J. Biol. Chem.* **263**, 9499-9501.

41. Howard, A. J., Gilliland, G.L., Finzel, B.C., and Poulos, T.L., *J. Applied Crystal.* **20**, 383.
42. Otwinowski, Z. (1991) In *Isomorphous Replacement and Anomalous Scattering: Proceedings of the CCP4 Study Weekend 25-26 January 1991* (Wolf, W., Evans, P.R., and Leslie, A.G.W., eds), pp. 80-86, SERC, Daresbury Laboratory, Warrington.
43. Brunger, A.T., Kuriyan, J., and Karplus, M. (1987) *Science* **235**, 458-460.
44. Finzel, B.C. (1987) *J. Applied Crystal.* **20**, 53-55.
45. Stein, P.E., Boodhoo, A., Tyrell, G.J., Brunton, J.L., and Read, R.J. (1992) *Nature* **355**, 748-750.
46. Ramachandran, G.N., and Sasisekharan (1968) *Adv. Protein Chem.* **23**, 283-438.
47. Mekalanos, JJ., Swartz, D.J., Pearson, G.D.N., Harford, N., Groyne, F., and De Wilde, M. (1983) *Nature* **306**, 551-557.
48. Kurosky, A., Markel, D.E., Peterson, J.W. (1977) *J. Biol. Chem.* **252**, 7257-7264.
49. Tsuji, T., Honda, T., Miwatani, T., Wakabayashi, T., and Matsubara, H. (1984) *FEMS Microbiol. Lett.* **25**, 243-246.
50. Lai, C.-Y. (1977) *J. Biol. Chem.* **252**, 7249-7256.
51. Olsvik, O., Wahlberg, J., Petterson, B., Uhlen, M., Popovic, T., Wachsmuth, I.K., and Fields, P.I. (1993) *J. Clin. Microbiol.* **31**, 22-25.
52. Dallas, W.S., and Falkow, S. (1980) *Nature* **288**, 499-501.
53. Leong, J., Vinal, A.C., and Dallas, W.S. (1985) *Infect. Immuno.* **48**, 73-77.
54. Yamamoto, T., and Yokota, T. (1983) *J. Bacteriol.* **155**, 728-733.
55. Tsuji, T., and Matsubara, H. (1987) *Microb. Pathol.* **2**, 381-390.
56. Lesk, A. (1989) Acta Crystall. *B* **106**, 106-118.
57. Sixma, T.K., Pronk, S.E., Kalk, K.H., van Zenten, B.A.M., Berhuis, A.M., and Hol, W.J.G. (1992) *Nature* **355**, 561-564.
58. Sixma, T.K., Stein, P.E., Hol, W.G.J., and Read, R.J. (1993) *Biochemistry* **32**,191-198.
59. Locht, C., and Keith, J.M. (1986) *Science* **232**, 1258-1264.
60. Nicosia, A., Perugini, M., Franzini, C., Casagli, M.C., Borri, M.G., Antoni, G., Almoni, M., Neri, P., Ratti, P. and Rappuoli, R. (1986) *Proc. Natl. Acad. Sci. U.S.A.* **83**, 4631-4635.
61. Murzin, A.G. (1993) *EMBO J.* **12**, 861-867.
62. Fukuta, S., Magnani, J.L., Twiddy, E.M., Holmes, R.K., and Ginsburg, V. (1988) *Infect. Immunol.* **56**, 1748-1753.
63. Gill, D.M., and King, C.A. (1975) *J. Biol. Chem.* **250**, 6424-6432.
64. Presta, L.G., and Rose, G.D. (1988) *Science* 240, 1632-1641.
65. Fairmain, R., Shoemaker, K.R., York, E.J., Stewart, J.M., and Baldwin, R.L., *Proteins: Struc., Funct., and Genetics* **5**, 1.
66. Streatfield, S.J., Sandkvist, M., Sixma, T.K., Bagdasarian, M., Hol, W.G., and Hirst, T.R. (1992) *Proc. Natl. Acad. Sci. U.S.A.* **89**, 12140-12144.
67. Hirst, T.R., and Holmgren, J. (1987) *Proc. Natl. Acad. Sci. U.S.A.* **84**, 7418-7422.
68. Hardy, S.J.S., Holmgren, J.,Johansson, S., Sanchez, J., and Hirst, T.R. (1988) *Proc. Natl. Acad. Sci. U.S.A.* **85**, 7109-7113.
69. Hofstra, H., and Witholt, B. (1985) *J. Biol. Chem.* **260**, 16037-16044.
70. De Wolf, M.J.S., Van Dessel, G.A.F., Lagrou, A.R., Hilderson, H.J.J., and Dierick, W.S.H. (1987) *Biochemistry* **26**, 3799-3806.
71. Surewicz, W.K., Leddy, J.J., and Mantsch, H.H. (1990) *Biochemistry* **29**, 8106-8111.
72. Schon, A., and Freire, E. (1989) *Biochem.* **28**, 5019-5024.
73. Lockman, H., and Kaper, J.B. (1983) *J. Biol. Chem.* **258**, 13722-13726.
74. Mosser, G., Mallouh, V., and Brisson, A. (1992) *J. Mol. Biol.* **226**, 23-28.
75. Tomasi, M., and Montecucco, C. (1981) *J. Biol. Chem.* **256**, 11177-11181.
76. Wisnieski, B.J., and Bramhall, J.S. (1981) *Nature* **289**, 319-321.
77. Tosteson, M.D., and Tosteson, D.C. (1978) *Nature* **275**, 142.
78. Krasilnekov, O.V., Muratkhodjaev, J.N., Voronov, A.E., and Yezepchuk, Y.V., (1991) *Biochim.*
79. Ribi, H.O., Ludwig, D.S., Mercer, K.L., Schoolnik, G.K., and Kornberg, R.D. (1988) *Science* **239**, 1272-1276.
80. Yang, J., Tamm, L.K., Tillack, T.W., and Shao, Z. (1993) *J. Mol. Biol.* **229**, 286-290.
81. Ludwig, D.S., Ribi, H.O., Schoolnik, G.K., and Kornberg, R.D. (1986) *Proc. Natl. Acad. Sci. USA* **83**, 8585-8588.
82. Masserini, M., Freire, M., Palestini, P., Calappi, E., and Tettamanti, G. (1992) *Biochem.* **31**, 2422-2426.
83. De Wolf, M.J.S., Fridkin, M., and Kohn, L.D. (1981) *J. Biol. Chem.* **256**, 5489-5496.

84. Goins, B., and Freire, E. (1988) *Biochem.* **27**, 2046-2052.
85. Bhakuni, V., Xie, D., and Freire, E. (1991) *Biochem.* **30**, 5055-5060.
86. Fishman, P.H., Moss, J., and Osborne, J.C. Jr. (1978) *Biochemistry* **17**, 711-716.
87. Sattler, J., Schwarzmann, G., Knack, I., Rohm, K.-H., and Wiegandt, H. (1978) *Hoppe-Seyler's Z. Physiol. Chem.* **359**, 719-723.
88. Jobling, M.G., and Holmes, R.K. (1991) *Mol. Microbiol.* **5**, 1755-1767.
89. Dallas, W.S. (1983) *Infect. Immun.* **40**:647-652.
90. Donta, S.T., Poindexter, N.J., and Ginsberg, B.H. (1982) *Biochem.* **21**, 660-664.
91. Holmgren, J., Fredman, P., Lindbald, M., Svennerholm, A.-M., and Svennerholm, L. (1982) *Infect. Immunol.* **38**, 424-433.
92. Critchley, D.R., Magnani, J.L., and Fishman, P.H. (1981) *J. Biol. Chem.* **256**, 8724-8731.
93. Brunton, J.L. (1990) In *The Bacteria* (Iglewski, B., and Clark, U., eds.), vol. **11**, 377-397, Academic Press, N.Y..
94. Orlandi, P.A., and Fishman, P.H. (1993) *J. Biol. Chem.* **268**, 17038-17044.
95. Lewis, M.J., and Pelham, H.R.B. (1990) *Nature* **348**, 162-163.
96. Rothman, J.E. and Orci, L. (1992) *Nature* **355**, 409-415.
97. Joseph, K.C., Kim, S.U., Steiber, A., and Gonatas, N.K. (1978) *Proc. Natl. Acad. Sci. U.S.A.* **75**, 2815-2819.
98. Joseph, K.C., Steiber, A., and Gonatas, N.K. (1979) *J. Cell Biol.* **81**, 543-554.
99. Tran, D., Carpentier, J.-L., Sawano, F., Gorden, P., and Orci, L. (1987) *Proc. Natl. Acad. Sci. U.S.A.* **84**, 7957-7961.
100. Svennerholm, A.-M., Sack, D.A., Holmgren, J., and Bardhan, P.K. (1982) *Lancet* **I**, 305-308.
101. De Aizpurua, H.J., Russell-Jones, G.J. (1988) *J. Exp. Med.* **167**, 440-451.
102. Chen, K.S., and Stroyer, W. (1990) *Eur. J. Immuno.* **20**, 443-446.
103. Elson, C.O., and Ealding, W. (1984) *J. Immunol.* **132**, 2736-2741.
104. McKenzie, McKenzie, S.J., and Halsey, J.F. (1984) *J. Immunol.* **133**, 1818-1823.
105. Guyon-Gruaz, A., Delmas, A., Pedoussant, S., Halimi, H., Milhaud, G., Raulais, D., and Rivaille, P. (1986) *Eur. J. Biochem.* **159**, 525-528.
106. Qu, Z.H., and Finkelstein, R.A. (1993) *Electrophoresis* **14**, 899-901.
107. Takeda, Y., Honda, T., Sima, H., Tsuji, T., and Miwatani, T. (1988) *FEMS Microbiol. Lett.* **49**, 7-11.
108. Finkelstein, R.A., Burks, M.F., Zupan, A., Dallas, W.S., Jacob, C.O., and Ludwig, D.S. (1987) *Rev. Infect. Dis.* **9**, 544-561.
109. Shoham, M. (1993) *J. Mol. Biol.* **232**, 1169-1175.
110. Jacob, C.O., Sela, M., Pines, M., Hurwitz, S., and Arnon, R. (1984) *Proc. Natl. Acad. Sci. U.S.A.* **81**, 7893-7896.
111. Anglister, J., and Zilber, B. (1990) *Biochemistry* **29**, 921-928.
112. Richards, F.M., and Kundrot, C.E. (1988) *Proteins: Struc., Funct., Genetics* **3**, 71-84.
113. Thompson, T.E., and Tillack, T.W. (1985) *Ann. Rev. Biophys. Chem.* **14**, 361-386.
114. McDaniel, R.V., and McIntosh, T.J. (1986) *Biophys. J.* **49**, 94-96.